Journal of Engineering Physics and Thermophysics, Vol. 79, No. 6, 2006

GASDYNAMIC PROCESSES AND HEAT TRANSFER IN THE CHANNELS OF SYSTEMS FOR EJECTION OF ELECTRON BEAMS FROM A VACUUM TO DENSE MEDIA

G. V. Konyukhov[a] and A. A. Koroteev[b]

UDC 536.2:532/533:532.72; 66.021.3

The complex problem on the dynamics of a gas flow and the heat transfer between it and the walls of the channels of systems for transport of electron beams has been solved.

The diagram of an electron-beam transport system (EBTS) designed for ejection of electrons from a vacuum to a region with a higher pressure, as high as the atmospheric pressure, is shown in Fig. 1. An electron beam that can be generated only in a vacuum passes through the stages with a consequently increasing pressure, connected by channels (diaphragms) with through holes. In each stage, the required rarefaction is provided by the pumping of the gas flowing from the more dense medium to meet the electron beam.

Such systems are usually supplied with additional elements for decreasing the scattering of electrons, the gas inflow, and the cooling of the diaphragms. We investigated an improved variant of beam ejection systems (Fig. 2), in which the stages are separated by partitions with a hole drilled by a beam at the beginning of its transport [1]. In the system being considered, the channels of minimum diameter were formed in a thermostable graphite possessing sublimation properties. This system features the following main advantages: the path of ejection of electrons is small in length, an electron beam can be focused and controlled, deviations of the electron-beam trajectory from the axis of the channel are small, and the gas inflow into the low-pressure stages is small.

The connecting channels are the most important units of an EBTS. These channels, passing large heat flows from the scattered electrons and the heated gas, should restrict the gas inflow into the stages with a lower pressure and, in doing so, should not distort the electron beam significantly. The most complex processes arise in the diaphragms connecting the regions with a relatively high pressure because, in them, the electron beam is scattered and the gas is rapidly heated.

Method for Investigating the Processes Occurring in the Channels of an EBTS. We will consider a region [Fig. 3] including channel ABCD of the diaphragm connecting the pressure stages 1 and 2 and the parts of these stages bounded by cylinders FHKD and NMEA with a radius $r = R_c$ exceeding the radius of the channel $r = r_c$. A magnetic field is formed by solenoid FS. An electron beam of radius $R_{e.b}$ is transported in the direction of increasing pressure (from stage 1 to stage 2). A gas jet propagates to meet the electron beam. A cylindrical coordinate system, in which the x axis is coincident with the axis of the channel and the r axis is directed along the radius, is introduced. The penetrable facing boundaries of the region being considered are formed by elements of the coordinate planes $x = 0$ (boundary HK) and $x = L$ (boundary NM). The following system of equations is used in calculations:

$$\frac{\partial \rho}{\partial t} + u\frac{\partial \rho}{\partial x} + v\frac{\partial \rho}{\partial r} + \rho\left[\frac{\partial u}{\partial x} + \frac{1}{r}\frac{\partial (rv)}{\partial r}\right] = 0 ,$$

$$\frac{\partial u}{\partial t} + u\frac{\partial u}{\partial x} + v\frac{\partial u}{\partial r} + \frac{1}{k^*}\left[\frac{T}{\rho}\frac{\partial (R\rho)}{\partial x} + \frac{R}{c_p}\frac{\partial h}{\partial x}\right] - \frac{1}{\mathrm{Re}\,\rho}\left(\frac{4}{3}\frac{\partial}{\partial x}\mu\frac{\partial u}{\partial x} - \frac{1}{r}\frac{\partial}{\partial r}r\mu\frac{\partial u}{\partial r}\right) =$$

[a]M. V. Keldysh Research Center, 8 Onezhskaya Str., Moscow, 125438, Russia; email: konyukhov@kerc.msk.ru; [b]Moscow Aviation Institute (State Technical University), 4 Volokolamsk Highway, Moscow, 125933, Russia. Translated from Inzhenerno-Fizicheskii Zhurnal, Vol. 79, No. 6, pp. 16–22, November–December, 2006. Original article submitted December 27, 2005.

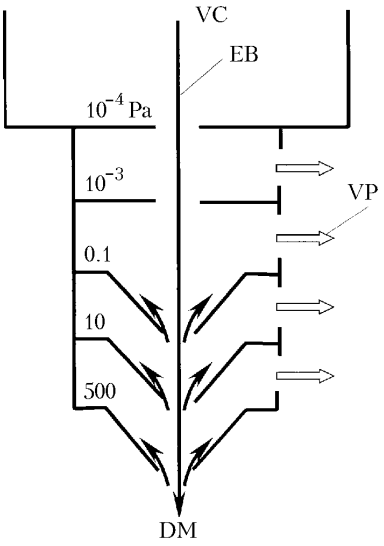

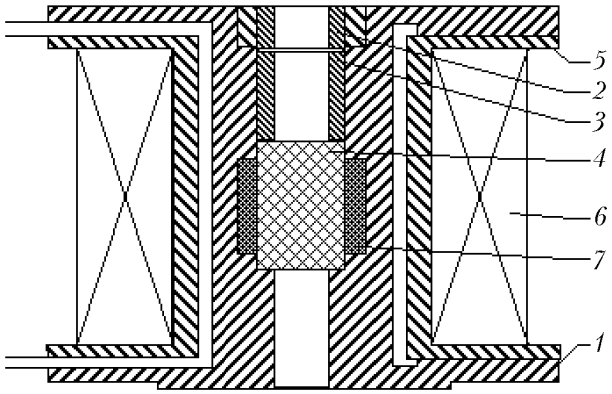

Fig. 1. Diagram of an EBTS with pressure stages placed in series: EB) electron beam; VC) vacuum chamber; VP) vacuum pumps; DM) dense medium (atmosphere).

Fig. 2. Beam ejection system: 1) pulley fork; 2) nut; 3) bush; 4) diaphragm; 5) frame; 6) focusing solenoid; 7) seal.

$$= \frac{1}{\mathrm{Re}\,\rho}\left[\frac{1}{r}\frac{\partial}{\partial r} r\mu \frac{\partial v}{\partial x} - \frac{2}{3}\frac{\partial}{\partial x}\frac{\mu}{r}\frac{\partial (rv)}{\partial r}\right], \tag{1}$$

$$\frac{\partial v}{\partial t} + u\frac{\partial v}{\partial x} + v\frac{\partial v}{\partial r} + \frac{1}{k^*}\left[\frac{T}{\rho}\frac{\partial (R\rho)}{\partial r} + \frac{R}{c_p}\frac{\partial h}{\partial r}\right] - \frac{1}{\mathrm{Re}\,\rho}\left(\frac{\partial}{\partial x}\mu\frac{\partial v}{\partial x} - \frac{4}{3}\frac{1}{r}\frac{\partial}{\partial r} r\mu\frac{\partial v}{\partial r}\right) =$$

$$= \frac{1}{\mathrm{Re}\,\rho}\left[\frac{\partial}{\partial x}\mu\frac{\partial u}{\partial r} - \frac{2}{3}\frac{\partial}{\partial r}\mu\frac{\partial u}{\partial x} - 2v\left(\frac{\mu}{r^2} + \frac{1}{3}\frac{\partial}{\partial r}\frac{\mu}{r}\right)\right],$$

$$\frac{\partial h}{\partial t} + u\frac{\partial h}{\partial x} + v\frac{\partial h}{\partial r} + \frac{k^* - 1}{k^*} kRT\left[\frac{\partial u}{\partial x} + \frac{1}{r}\frac{\partial (rv)}{\partial r}\right] - \frac{k}{\mathrm{Re}\,\rho}\left(\frac{\partial}{\partial x}\frac{\mu}{\mathrm{Pr}}\frac{\partial h}{\partial x} + \frac{1}{r}\frac{\partial}{\partial r}\frac{r\mu}{\mathrm{Pr}}\frac{\partial h}{\partial r}\right) =$$

$$= \frac{2(k^* - 1)\,\mu k}{\mathrm{Re}\,\rho}\left\{\left(\frac{\partial u}{\partial x}\right)^2 + \left(\frac{\partial v}{\partial r}\right)^2 + \frac{v^2}{r^2} + \frac{1}{2}\left(\frac{\partial u}{\partial r} + \frac{\partial v}{\partial x}\right)^2 - \frac{1}{3}\left[\frac{\partial u}{\partial x} + \frac{1}{r}\frac{\partial (rv)}{\partial r}\right]^2\right\} + \frac{(k^* - 1)\, r_c}{a^{*3}\rho^*\rho} kq_v,$$

$$dh = c_p dT, \quad \mu = \mu(h), \quad c_p = c_p(h), \quad k = k(h), \quad \mathrm{Pr} = \mathrm{Pr}(h), \quad R = R(h),$$

$$q_v = (N/(EF))\,(dE/dx), \quad F = \pi R_{e.b}^2.$$

System (1) is written in the dimensionless form; the dimensionless variables are related to the dimensional ones (having the interlinear index "dim") by the following relations: $x = x_{dim}/r_c$, $r = r_{dim}/r_c$, $t = t_{dim}a^*/r_c$, $\rho = \rho_{dim}/\rho^*$, $u = u_{dim}/a^*$, $v = v_{dim}/a^*$, $h = h_{dim}/h^*$, $T = T_{dim}/T^*$, $\mu = \mu_{dim}/\mu^*$, $c_p = (c_p)_{dim}/c_p^*$, $R = R_{dim}/R^*$. The radial coordinate of the wall of the channel $r_w = 1$.

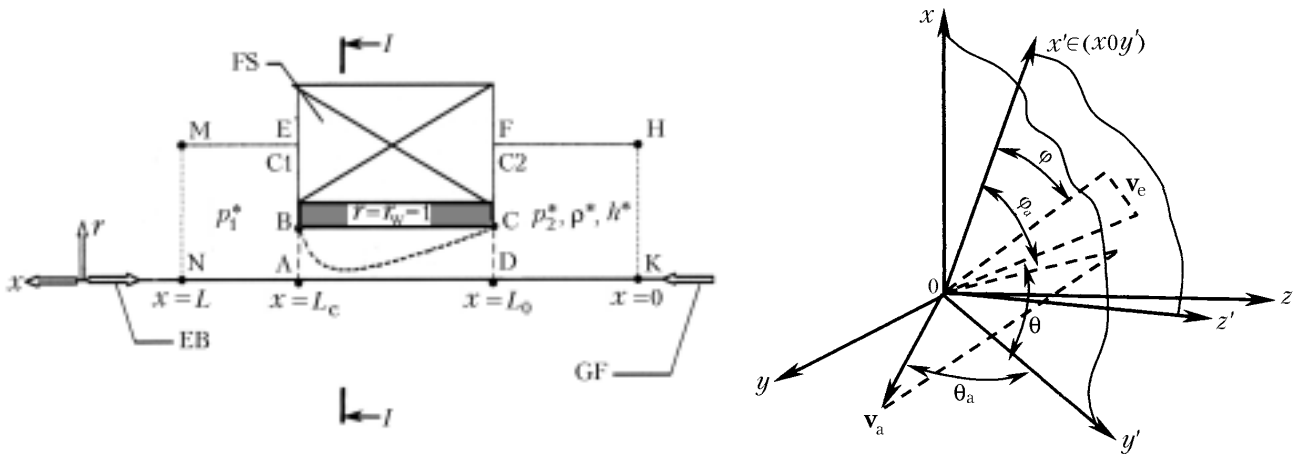

Fig. 3. Diagram of the computational region: FS) focusing solenoid; C1) pressure stage 1; C2) pressure stage 2; EB) electron beam; GF) gas flow.

Fig. 4. Coordinate system for investigating the interaction of an electron beam with a gas flow.

It is assumed that the energy lost by the electrons of a beam as a result of their inelastic collisions with the atoms of a medium is expended for increasing the internal energy of the gas flow. The loss in the electron energy is calculated by the Bethe–Bloch slowing-down theory:

$$\frac{dE}{dx} = 2.46 \cdot 10^{-15} \frac{Z}{A} \beta^{-2} \rho \left[\ln \frac{\gamma(\gamma+2)}{2\,(I/(m_e c^2))^2} + 1 - \beta^2 + 0.125\gamma^2 - (2\alpha+1)\ln 2 \right]. \tag{2}$$

The magnetogasdynamic effects have no a significant influence on the gas flow: the Stuart number characterizing these effects does not exceed 0.004 in this case.

It is assumed that the gas flow at the input (cross section HK in Fig. 3) of the channel is uniform and the acceleration of the gas to this cross section is performed isentropically. The density and enthalpy of the decelerated gas at the input cross section of the channel are determined and the conditions under which a transverse motion of the gas at this cross section is absent are set. The u component of the gas flow velocity at cross section HK is calculated using the procedure of determining the steady-state regime of flow:

$$\int_0^{R_c} \rho\,(0, r)\, u\,(0, r)\, r dr = \int_0^1 \rho\,(L_c, r)\, u\,(L_c, r)\, r dr\,. \tag{3}$$

The symmetry conditions are set at the axis of the flow, the adhesion conditions are set for the velocity components at boundaries HF, FC, CB, and BE, and the first-kind or the second-kind conditions are set for the enthalpy. If a rarefied gas flows in the channel, the conditions at broken line HFCBE are determined with account for the slipping and the temperature jump at the channel wall. The "controllable" boundary conditions are set at boundaries ME and EN: at $M < 1$, the pressure at these boundaries is equal to the pressure p_1 in stage 1 from which an electron beam is ejected; at $M \geq 1$, this pressure is independent of p_1. The conditions that the second derivative of the pressure with respect to the normal to the corresponding surface is equal to zero were used for determining the velocity components and the enthalpy at boundaries EM and MN and the flow density at local values of $M \geq 1$.

The system of equations (1) was solved using the procedure of splitting of the equations by physical processes and spatial directions; the stationary field of thermal and gasdynamic quantities was determined by the ascertainment method.

The interaction of the gas in the channel with an electron beam was investigated in the coordinate systems shown in Fig. 4. The z axis of the fixed coordinate system coincides with the symmetry axis and points in the direc-

tion of propagation of the electron beam. The x and y axes are directed radially, and the system as a whole represents a right triple. The y' axis of the system, associated with the direction of the electron beam, is coincident with the velocity vector $\mathbf{v}_e$ of an electron before its collision with an atom, the x' is perpendicular to the y' axis and lies in the $x0y'$ plane, and the z' axis completes the system to the right triple. The angle between the projection of $\mathbf{v}_e'$ on the $x'0z'$ plane and the $0x'$ axis will be denoted by φ, and the angle between the projection of $\mathbf{v}_a$ on the $x'0z'$ plane and the $0x'$ axis will be denoted by φ_a.

The coordinates and velocities of electrons at the input of the computational region (cross section NM in Fig. 3) are determined as

$$x = r_c (\Gamma_1)^{1/2} \cos(2\pi\Gamma_2), \quad y = r_c (\Gamma_1)^{1/2} \sin(2\pi\Gamma_2), \quad v_{ex} = v_{ey} = 0; \quad v_{ez} = v_{e0} \text{ at } z = 0, \tag{4}$$

where v_{ex}, v_{ey}, and v_{ez} are the projections of $\mathbf{v}_e$ on the x, y, and z axes.

The time between the collisions (the time of the free electron motion) τ_{col} is determined from the equation

$$\frac{d\psi}{dt} = -n_a v_e \int_0^{\pi} \sigma(\theta, v_e)\, d\theta, \quad \psi(0) = 0. \tag{5}$$

For determining the value of τ_{col}, the logarithm of the random number Γ_3 distributed homogeneously in the interval (0, 1) is calculated, and then the condition $\psi(\varphi) = \ln \Gamma_3$ is realized:

$$\tau_{col} = -\frac{\ln \Gamma_3}{n_a v_e \int_0^{\pi} \sigma(\theta, v_e)\, d\theta}. \tag{6}$$

The path of free electron motion is calculated without regard for the eigenfield of the electron beam

$$\frac{d}{dt}\mathbf{p}_e = e[\mathbf{v}_e \times \mathbf{B}], \quad \text{at } t = 0: \ \mathbf{r}_e = \mathbf{r}_{e0}; \quad \mathbf{p}_e = \mathbf{p}_{e0}. \tag{7}$$

On the assumption that the velocity distribution of the gas molecules represents a Maxwell function, the probability density of this distribution over φ_a and θ_a will be equal to $P_1(\varphi_a) = 1/(2\pi)$ and $P_2(\theta_a) = 1/(2 \sin \theta_a)$. The random value of the velocity v_a of an atom colliding with an electron is determined by the Neumann method in accordance with the conditional probability density of this value equal to

$$P_3\left(\frac{v_a}{v_e}, \theta_a\right) = \frac{4 \exp(-Dv_a^2)\, Dv_a^2 \sqrt{D\left(v_e^2 + v_a^2 - 2v_e v_a \cos\theta_a\right)}}{\exp(-Dv_e^2) + \frac{1}{\sqrt{D}\, v_e}\left(2Dv_e^2 + 1\right) \int_0^{\sqrt{D} v_e} \exp(-x^2)\, dx}, \quad D = m_a/(2k_B T_{dim}). \tag{8}$$

Here, T_{dim} are the gas temperature, K.

The velocity of an electron after its collision with an atom is determined using the laws of momentum and energy conservation. Then the time to the next collision and the coordinates of a new collision are calculated. In this way, the collisionless path of an electron and its interaction characteristics are determined. Calculations are repeated as long as the electron loses its energy or leaves the computational region. For investigating the propagation of an electron beam in a gas flow, corrections accounting for the characteristics of the flow are introduced.

The loss in energy of the electron beam and the changes in the direction of its propagation, in the radius of the beam, and in other its parameters are determined by averaging the corresponding characteristics determined for an ensemble of electrons.

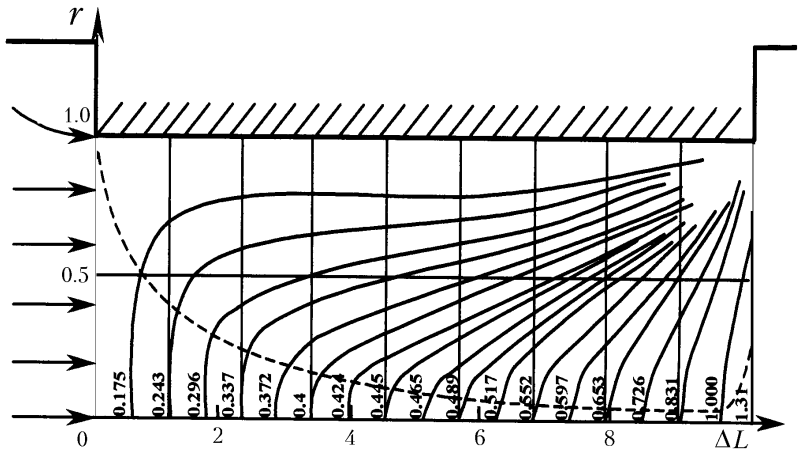

Fig. 5. Lines of constant Mach numbers of the gas flow in a channel of length $\Delta L = 10$ at $N = 30$ kW.

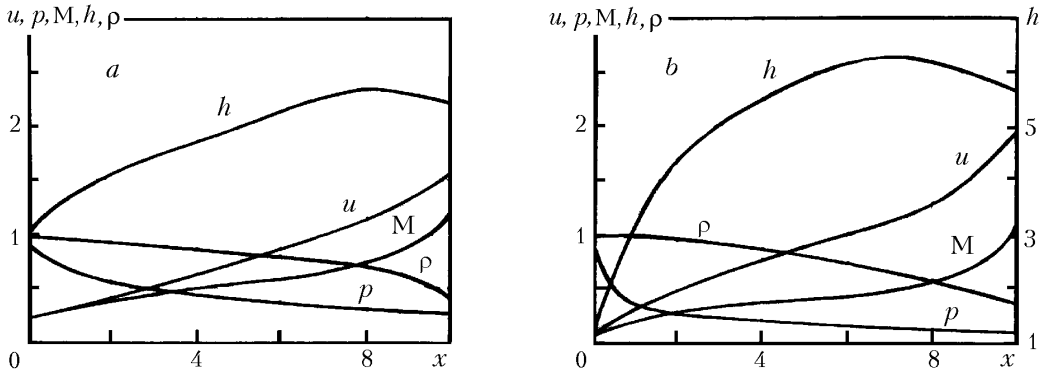

Fig. 6. Change in the density, velocity component, enthalpy, pressure, and Mach number at the axis of the channel of length $\Delta L = 10$ in the case of transport of an electron beam to the region with a pressure of $1.3 \cdot 10^3$ Pa: $N =$ 10 kW (a) and 50 (b).

Results of Calculations and Discussion. In the calculations carried out with the use of system (1), the following values of the parameters were used: $p_2^* = 1.33 \cdot 10^3$ Pa, $h_2^* = 3 \cdot 10^5$ J/kg, $\rho_2^* = 1.55 \cdot 10^{-2}$ kg/m^3, $\mu_2^* = 1.84 \cdot 10^{-5}$ Pa·sec, $r_c = 1$ mm, Re = 293, $E = 100$ keV, and $p_1 = 1$ Pa.

Figure 5 shows the lines of constant Mach numbers. The boundary layer is denoted by the dashed line. The coordinates of the cross sections being considered are plotted along the axis. Because of the suction of the boundary layer toward the low-pressure region, the flow in the central part of the channel is accelerated to M > 1. Figure 6 shows the longitudinal distributions of the density, the u component of the flow velocity, the enthalpy, the pressure, and the Mach number at the axis of the channel of length $\Delta L = 10$ for ejected electron beams of different powers. The gas in the channel is heated as a result of its interaction with electrons. The dependence of the maximum enthalpy h_{max} at the axis of the flow on the electron-beam power at $\Delta L = 10$ is illustrated in Fig. 7.

Even in the case of transport of powerful ($N = 50$ kW) beams through fairly long ($\Delta L = 10$) channels, the maximum enthalpy at the axis of the flow $h_{max} = 6.33$. The corresponding temperature $T_{max} = 5.7$ ($T_{max} = 1710$ K in the dimension form) does not exceed the sublimation temperature of the material of the channel wall. Under these conditions, the external cooling should provide only the removal of the heat flowing from the scattered electrons to the wall, which is determined by only the rate of widening of the electron beam. The possibility of appearance of chemical reactions between the heated gas and the wall material was not considered in the present work.

The change in the radius of an electron beam in a channel of an EBTS is illustrated in Fig. 8. The radius of the beam at the input of the channel of length $\Delta L = 15$ is equal to 1 mm. Curves for external magnetic fields of dif-

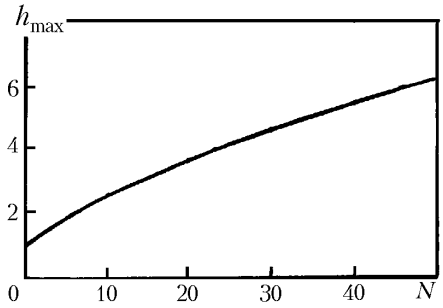

Fig. 7. Dependence of the maximum enthalpy of the gas at the axis of the gas flow on the power of the electron beam in the channel of length $\Delta L = 10$. N, kW.

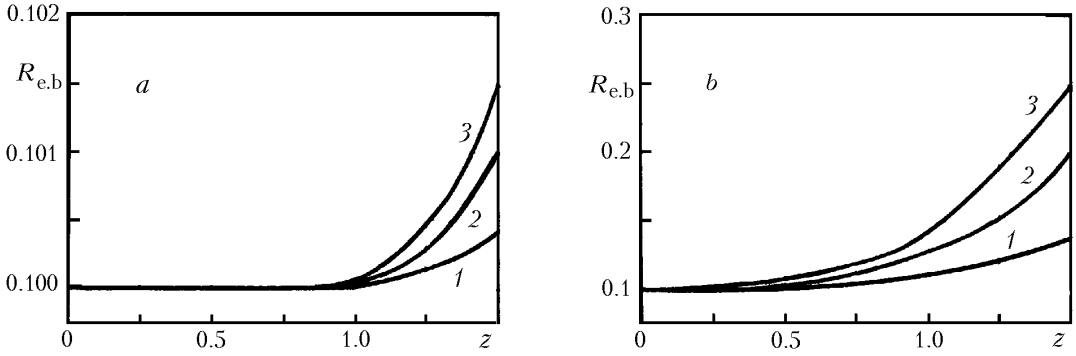

Fig. 8. Change in the radius of an electron beam in the channels of EBTSs [a) transport to the region with a pressure of 10^3 Pa, r_c = 1.015 mm; b) transport to the atmosphere, r_c = 2.7 mm) at a focusing-magnetic-field induction of 0.7 (1), 0.5 (2), and 0 T (3). $R_{e.b}$; z, cm.

ferent inductions are presented. Even if an electron beam is transported to a lower-pressure region through a fairly long channel, it is not scattered markedly. A different pattern was detected for atmospheric channels: electrons transported through long channels are subjected to a strong scattering. This makes the cooling of the walls of the channels difficult and leads to the appearance of a large loss in the energy of the electron beam. That is why small-length channels are used for transport of electrons to the atmosphere and this transport is performed at high Reynolds numbers of the gas flow because, in this case, a thin boundary layer arises. In the case where the ratio between the geometry of a channel and the power of a beam is such that the gas is not heated to the temperature at which the channel-wall material breaks down (i.e., when there is no need to calculate the heat transfer between the gas and the channel wall), the flow in this channel can be approximately calculated with the use of equations for a nonviscous and thermally nonconductive liquid with constant thermophysical properties. If, in this case, the transverse motion of the gas in the channel is disregarded, an analytical solution can be obtained from a simplified system of equations obtained in [2]. Analysis of the results of a large number of test calculations allowed us to determine the optimum length L_{opt} of diaphragms through which electrons are transported to the atmosphere:

$$L_{opt} = (3 - 5) \cdot \frac{9.1 \cdot 10^{-4}}{\bar{\rho}}. \qquad (9)$$

The cooling of the wall of a channel for transport of an electron beam should be sufficient for removal of the heat flow that is due to the scattering of the electrons falling on the channel wall. The maximum value of this heat flow can be estimated on the assumption that the electron-beam energy transferred within the outer ring (cut by the wall) is completely absorbed by the material of the channel wall and is converted into the heat energy.

One of the main features of a gas flow in a channel of an EBTS is a much lower velocity of the gas flowing into a stage, as compared to that in the case where a heat release is absent, all other things being equal. The effect of

decreasing the flow rate of the gas is attained due to the rapid heating of the gas by electrons. This effect should be used in the fullest measure for improvement of the operating parameters of the EBTS and for decreasing its weight and dimensions. When the gas flow is heated to a high temperature (h_{max} = 6–7), its rate decreases by four to five times. Since channels used for transport of electrons to the atmosphere have a limited length, the decrease in the gas flow into them is manifested not as significantly as in the case of transport of electrons to a rarefied gas.

CONCLUSIONS

1. The method proposed allows one to investigate the dynamics of a gas flow in a channel of an EBTS with pressure stages placed in series and the heat transfer between this flow and the walls of the channel.

2. It was established that the most important characteristics of the channels of EBTSs, representing their main and most heat-loaded elements, are the existence of a sonic surface inside the channel, the possibility of propagation of a supersonic gas flow in it, and the pronounced effect of decreasing the gas flow rate in the process of ejection of an electron beam.

3. Optimum regimes of functioning and cooling of the channels of EBTSs were recommended.

NOTATION

A, atomic mass; $a^* = (k^* R^* T^*)^{1/2}$, velocity of sound of the decelerated gas, m/sec; $\mathbf{B}$, magnetic-induction vector, T; c, velocity of light in a free space; c_p, specific heat at a constant pressure; c_p^*, specific heat of the decelerated gas at a constant pressure; E, electron energy, J; e, electron charge, C; I, ionization potential of the scattering medium, J; h, enthalpy; h^*, enthalpy of the decelerated gas; h_{max}, maximum enthalpy; k, adiabatic index; k^*, adiabatic index of the decelerated gas flow; k_B, Boltzmann constant; L, dimensionless length of the computational region; L_{opt}, optimum length of a channel, m; ΔL, dimensionless length of the channel; L_0, dimensionless coordinate; L_c, dimensionless coordinate of the output (for the gas) cross section of the channel; M, Mach number; m_a, atomic mass, kg; m_e, electron mass, kg; N, power of an electron beam; n_a, concentration of atoms; P, probability density; Pr, Prandtl number; p, pressure; $\mathbf{p}_e$, electron momentum, kg·m/sec; $\mathbf{p}_{e0}$, electron momentum at the initial instant of time, kg·m/sec; q_v, heat released by an electron beam, W/m^3; R, gas constant; R^*, gas constant of the decelerated gas; R_c, outer radius of the computational region; $R_{e.b}$, radius of the electron beam, cm; r, radial coordinate; r_w, radial boundary of the channel; r_c, radius of the channel, m; $\mathbf{r}_e$, radius-vector of the electron coordinate; $\mathbf{r}_{e0}$, radius-vector of the electron coordinate at the initial instant of time; $\mathrm{Re} = \rho^* a^* r_c/\mu^*$, Reynolds number; T, dimensionless temperature; T^*, dimensionless temperature of the decelerated gas; T_{max}, maximum dimensionless temperature; t, time; u, axial component of the gas velocity; x, longitudinal coordinate; Z, nuclear charge, 1/m^3; v, radial component of the gas velocity; $\mathbf{v}_a$ and v_a, velocity vector of an atom before the collision and its magnitude, m/sec; $\mathbf{v}_e$ and v_e, velocity vector of an electron and its magnitude, m/sec; α, ratio between the kinetic energy of an electron and its rest energy; β, ratio between the velocity of an electron and the velocity of light; Γ, random number distributed uniformly over the interval [0, 1]; γ, electron energy in terms of $m_e c^2$; μ, dynamic viscosity; θ, angle of electron scattering; θ_a, angle between the velocity vectors of an electron and the atom on which it is scattered; ρ, density; ρ^*, density of the decelerated gas; $\bar{\rho}$, averaged density of the gas in the channel, kg/m^3; σ, elastic-scattering cross section; τ_{col}, time of free electron motion (between two collisions), sec. Subscripts: a, atom; e, electron; max, maximum; v, heat release per unit volume; w, radial boundary of the computational region or the channel; dim, dimensional quantity; col, parameter characterizing the change in the corresponding physical quantity between the two last collisions of an electron with atoms; e.b, electron beam; 0, initial moment of time; 1, and 2, low- and high-vacuum pressure stages; *, decelerated gas; ′, coordinate system related to the direction of electron motion; opt, optimum.

REFERENCES

1. M. N. Vasil'ev and A. S. Koroteev, An apparatus for ejecting a concentrated electron beam into a gaseous medium, *Prib. Tekh. Eksp.*, No. 1, 154–161 (1984).
2. A. A. Koroteev, *Small-Size Power-Intensive Systems for Transport of Electron Beams into Dense Media* [in Russian], Mashinostroenie, Moscow (2003).